Heliyon 9 (2023) e16260

Contents lists available at ScienceDirect

Heliyon

journal homepage: www.cell.com/heliyon

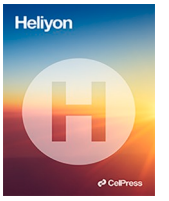

Research article

Emission impacts of left-turn lane on light-heavy-duty mixed traffic in signalized intersections: Optimization and empirical analysis

Jieyu Fan [a], Aoyong Li [b,**], Anugrah Ilahi [c], Kun Gao [d,*]

[a] Faculty of Engineering, Computer Science and Psychology, Department of Human Factors, Ulm University, Ulm, 89069, Germany
[b] State Key Laboratory of Automotive Safety & Energy, School of Vehicle and Mobility, Tsinghua University, Beijing, 115003, China
[c] Institute for Transport Studies, University of Natural Resources and Life Sciences (BOKU), 1190, Vienna, Austria
[d] Department of Architecture and Civil Engineering, Chalmers University of Technology, 412 96, Goteborg, Sweden

ARTICLE INFO

Keywords:
Traffic emission
Instantaneous emission model
Left-turn lane
Traffic efficiency and simulation

ABSTRACT

Reducing emissions from the transport sector is one of the crucial countermeasures for climate action. This study focuses on the optimization and emission analysis regarding the impacts of left-turn lanes on the emissions of mixed traffic flow (CO, HC, and NO_x) with both heavy-duty vehicles (HDV) and light-duty vehicles (LDV) at urban intersections, combining high-resolution field emission data and simulation tools. Based on high-precision field emission data collected by Portable OBEAS-3000, this study first develops instantaneous emission models for HDV and LDV under various operating conditions. Then, a tailored model is formulated to determine the optimal left-lane length for mixed traffic. Afterward, we empirically validate the model and analyze the effect of the left-turn lane (before and after optimization) on the emissions at the intersections using the established emission models and VISSIM simulations. The proposed method can reduce CO, HC, and NO_x emissions crossing intersections by around 30% compared to the original scenario. The proposed method significantly reduces average traffic delays after optimization by 16.67% (North), 21.09% (South), 14.61% (West), and 2.68% (East) in different entrance directions. The maximum queue lengths decrease by 79.42%, 39.09%, and 37.02% in different directions. Even though HDVs account for only a minor traffic volume, they contribute the most to CO, HC, and NO_x emissions at the intersection. The optimality of the proposed method is validated through an enumeration process. Overall, the method provides useful guidance and design methods for traffic designers to alleviate traffic congestion and emissions at urban intersections by strengthening left-turn lanes and improving traffic efficiency.

1. Introduction

The transport sector takes up around a quarter of greenhouse gas (GHG) emissions globally and plays a crucial role in realizing the ultimate goal of net-zero emissions in the era of climate change [1,2]. Meanwhile, transport-related air pollution contributes to a large part of global air pollution [3,4]. Although air quality standards have been improved by government and agencies such as the US

* Corresponding author.
** Corresponding author.
E-mail addresses: aoyong@tsinghua.edu.cn (A. Li), gkun@chalmers.se (K. Gao).

https://doi.org/10.1016/j.heliyon.2023.e16260
Received 23 March 2023; Received in revised form 26 April 2023; Accepted 11 May 2023
Available online 16 May 2023

Environmental Protection Agency and the World Health Organization (WHO) to guide and facilitate air quality improvements, more than 90% of the world's population lives in areas where pollutant levels are higher than WHO air quality standards [5]. Excessive emissions in terms of GHG emissions and pollutants in the transport sector have been resulting in profound negative impacts on air quality, climate, and public health that influence almost every piece of daily life [6,7]. Especially, traffic congestion due to large traffic volume reduces driving speed and thus leads to significantly higher energy consumption and emissions during operations [8,9]. Therefore, it is crucial to reduce emissions in the transport sector by improving infrastructure, vehicles, and the operation of the systems from different aspects. Urban transport managers and policymakers worldwide are pressing to reduce transport emissions to fulfill the national target of reducing emissions.

One of the focuses of reducing transport emissions in urban areas is to reduce traffic congestion in typical bottlenecks (e.g., intersection and freeway merging areas) and corresponding traffic emissions, taking advantage of effective infrastructure and traffic management. In traffic congestion situations, internal combustion engine (ICE) vehicles emit 5–10 times more pollutants than in normal driving conditions [10]. One essential component for establishing effective infrastructure and traffic management to reduce traffic emissions is the use of vehicle emission models. These models quantify the emission patterns of vehicles under different driving conditions, providing important insights for reducing emissions and improving air quality. (e.g., speed and acceleration). Vehicle emission models are essential for evaluating and optimizing the actual performances of traffic management. The necessity of vehicle emission models has motivated researchers to develop various modeling approaches based on different data sources [11]. used a portable emission test system to test and examine the on-road fuel consumption and carbon dioxide (CO_2) emissions of 60 light passenger vehicles. Their results indicated that the on-road fuel consumption and emissions under the average driving patterns were 10 $\pm$ 2% higher than type-approval values and were highly influenced by speeds. Their results highlighted the necessity of measuring emissions in the type approval test based on real-world driving features [12]. studied traffic emissions in the work zone using the Comprehensive Modal Emissions Model (CMEM) to generate second-by-second emissions. They reported that fuel consumption rates and emission rates of hydrocarbons (HC), carbon monoxide (CO), nitrogen oxide (NO_x), and CO_2 were highly related to traffic conditions. Meanwhile, the emission patterns of light-duty and heavy-duty vehicles in different traffic conditions presented different principles. Meanwhile [13], developed a method for assessing the representativeness of fuel-specific vehicle-based emission factors. The method was validated based on actual emission data for 23 selected light gasoline vehicles. Results indicated that route average emission factors varied by approximately 20% for NO_x or CO, and site-specific emission factors varied by 20% for NO_x and 30% for CO between sites, respectively. However, fuel-based HC emission rates varied little with engine load, between routes, or between sites. This showed that estimating vehicle operational emissions was a complex process, especially in traffic flow with much complexity and randomness [14]. confirmed the importance of accurate emission modeling for different vehicle types (e.g., hybrid electric vehicles) in the Vehicle Specific Power model and improved the emission models tailored for hybrid electric vehicles. They also made significant improvements to the emissions detection tool in terms of temporal resolution, simultaneous data recording capability and data accuracy.

One of the most critical infrastructure and traffic management for reducing traffic emissions is optimizing the design of intersections [15–17], which are the most critical bottlenecks of urban transportation systems. To name a few [16], investigated the design of multiple target signal cycle lengths to minimize vehicle delays and traffic emissions. The simulation software INTEGRATION was used to simulate traffic demand distribution, traffic demand levels, signal timing loss times, and signal cycle lengths and to estimate intersection delays and emissions (CO_2, HC, CO, and NO_x) [18]. pointed out that emissions of road pollutants were related to many infrastructure parameters as well as to the intensity and type of traffic. They investigated the performances and the pollutant emissions of turbo roundabouts (CO, CO_2, CH_4, NO_x, PM2.5, and PM10), assessed by COPERT software (European emission calculation tool) [19]. studied road geometries that continuously guide drivers from the entrance to the exit while eliminating weaving and queue jumping, and investigated the impact of conventional single-lane and two-lane roundabouts on traffic emissions, traffic capacity, and safety. Their results showed that the implementation of turbo-roundabouts has no benefit in terms of reducing emissions.

In urban intersections, the lane functions are generally set to left-turn (or turnaround), through, and right-turn. The left-turn lane generates the most conflict points among vehicles from different directions and thus has the most significant impact on traffic efficiency and emissions [16,20,21]. When the left-turn traffic volume reaches a certain threshold, a dedicated left-turn lane is required to reduce the impact of left-turn vehicles in the opposite road lanes to improve traffic efficiency at the intersections [22]. Therefore, rationalizing the design of left-turn lanes is one of the most effective measures to improve traffic efficiency and reduce traffic emissions at intersections [15]. In the relevant studies of optimizing left-turn lanes, the main design objectives are generally to reduce conflict points and improve capacity and efficiency. For instance Ref. [23], developed a method to determine the length of left-turn lanes at signalized intersections that can prevent spillover. The study considered intersection capacity, arrival rates, different signal schemes, and sequences of left-turn and through traffic to obtain the probabilities of lane blockage and lane overflow to calculate the recommended length of left-turn lanes. Yao and Zhang (2013) proposed three models to optimally allocate lane space and green divisions for isolated signalized intersections with short left-turn lanes. Two performance metrics were proposed to compare the performance of the three models and to investigate their sensitivity to the model parameters. Afterward, Bing et al. (2014) investigated the impact of lane configurations on traffic emissions based on the traffic simulation tools VISSIM and VSP emission models. Traffic emissions under different lane configurations were analyzed in different scenarios in terms of five indicators, including average delay per vehicle, the average number of stops per vehicle, and total emissions of CO, HC, and NO_x. Results showed that the presence of dedicated left-turn lanes (with or without widening) had a significant impact on the traffic flow and emission characteristics of the intersection [24]. focused on improving the operation of urban intersections, which are often congested and a key bottleneck of the road network. The study proposes a model that integrates an improved optimal velocity model and a multi-intersection signal state function to analyze traffic flow, including vehicles turning left accurately. The model also considers pollutant emissions and has been tested through

simulation analysis to show its effectiveness in describing actual traffic flow [25]. proposed an optimization model for minimizing delay in traffic for left-turns at signalized intersections using exit-lanes for a left-turn (EFL) traffic organization. The model considered the relationship between the pre-signal start node of the EFL and the queuing dissipation time of left-turn vehicles. The validation of the model showed that a well-designed pre-signal control scheme can improve capacity and reduce emissions while minimizing average vehicle delays compared to conventional left-turn lanes.

There is extensive literature on the effects of left-turn lanes on traffic flow characteristics (e.g., travel time and speed) [26,27]. However, there is much less research about the impact of dedicated left-turn lane settings on different exhaust emissions. In particular, most existing studies ignored the complexity of mixed traffic flow with different vehicle types and mainly focused on single traffic flow with merely light-duty passenger vehicles. Few studies have investigated the left-turn lane optimization specific for mixed traffic flows, even though heavy-duty vehicles (HDVs) and light-duty vehicles (LDVs) have significantly distinct emission patterns, vehicular sizes, and kinetic characteristics [12–14]. Therefore, the left-turn lanes at the intersections for mixed traffic are anticipated to have different design principles and should be tailored based on new methods for mixed traffic rather than existing methods for LDVs.

To address the gap, this study focuses on the optimization and emission analysis regarding the impacts of left-turn lanes on the emissions (CO, HC, and NO_x) of mixed traffic flow with HDVs and LDVs, combining high-resolution field emission data and simulation tools. We utilize portable OBEAS-3000 to collect high-precision emission data for LDVs and HDVs in various traffic scenarios. Based on the field data, we first develop separate instantaneous emission models for HDVs and LDVs under various operating conditions. Then, we formulate a tailored optimization model to determine the optimal left-lane length considering the penetration rate of HDV and traffic volumes from different directions at the intersection. Finally, we empirically validate the proposed model and analyze the effect of the length of the left-turn lane (before and after optimization) on the emissions of mixed traffic flows based on the established emission model and microscopic traffic simulations using VISSIM.

The remaining sections of the paper are structured as follows. Section 2 provides a description of the emission data collection process and emission modeling. In Section 3, we elaborate on the model to determine the length of the left-turn lane for mixed traffic flow. Section 4 describes the simulation method and empirical case study, followed by concluding remarks in Section 5.

2. Emission data collection and emission model establishment

This study uses the portable emission monitoring device OBEAS-3000 to collect vehicle emission data regarding CO, HC, and NO_x in real traffic scenarios, considering the complexity of road conditions and the contingent nature of vehicle operating conditions. The instantaneous emission rate of CO, HC, and NO_x operating in different traffic conditions for LDV and HDV are collected to establish vehicle-type specific emission models.

2.1. Emission data collection equipment

The OBEAS-3000 portable emission monitor in Fig. 1 was used to continuously collect the instantaneous emission of CO, HC, NO_x, and corresponding vehicle operating dynamics, including positions (coordinates), speed, and accelerations. The data acquisition frequency is 10 Hz, namely, ten times in a second. The data reflect the quantitative relationship between instantaneous emissions and vehicle dynamics in a high resolution [28]. The experimental vehicles include both LDVs and HDVs. LDVs refer to M1, M2, and N1 vehicles with a total mass not exceeding 3.5 tonnes, while HDVs refer to vehicles with a total mass exceeding 8 tonnes [29]. The LDVs in this study were the Volkswagen Lavida and Harvard SUV, which were typical and popular household passenger cars in China. For HDVs, we used the vehicle of FAW Liberty. The petrol emission standards for the experimental vehicles were Chinese National IV, with engine displacements of 1.6 L (Volkswagen Lavida), 2.0 L (Harvard SUV), and 6.6 L for the HDV. The detailed parameters of the experimental LDVs and HDV are summarized in Table 1. The vehicles were driven in the urban contexts of Shanghai, China in the daytime to collect the emission data under real traffic conditions. After experiments, a total of 170972, 66804 and 52251 valid records were finally collected for Volkswagen Lavida, Harvard SUV, and the heavy-duty vehicle, respectively.

Fig. 1. OBEAS-3000 portable emission monitor.

Table 1
Technical details of the experimental vehicles.

Model/Parameters	Light vehicles		Heavy vehicles
Brands	Volkswagen Lavida	Harvard SUV	FAW Liberty
Mass (kg)	1285	1725	15790
Engine Displacement (L)	1.6	2.0	6.6
Fuel type	Petrol	Petrol	Diesel
Emission standards	State IV Standard	State IV Standard	State IV Standard
Year of manufacture	2010	2014	2012

2.2. Instantaneous vehicle emission models for light- and heavy-duty vehicles

The VSP calculation model can effectively describe the instantaneous emission characteristics of vehicles, and it has a higher time and driving state resolution than other macroscopic emission models, which can effectively express the time-varying characteristics of traffic emissions. Vehicle emission patterns depend highly on vehicle dynamics during operations, which is a complex process. In this study, we adopt the well-known Vehicle Specific Power (VSP) model to establish the relationship between vehicle dynamics and instantaneous emissions of different exhausts. Utilizing field data we have collected in Shanghai of China, we develop instantaneous emission models for both LDVs and HDVs in terms of CO, HC and NO_x for quantifying vehicle emissions. VSP is the instantaneous power per unit mass of a vehicle (kW/t), and the transient emissions of a vehicle are closely related to the VSP values [30]. It should be noted that the VSP models for vehicles in different countries may be different due to different vehicle emission standards. Herein, we use the field emission data in Shanghai for empirical analysis. The formula of VSP [31] can be seen in Eq. (1).

$$VSP = v \times (a + g \times grade + g \cdot C_R) + \frac{1}{2} \cdot \rho_a \cdot \frac{C_D}{m} \cdot A \cdot v^3 \tag{1}$$

where v is the instantaneous speed, m/s. a is the instantaneous acceleration, m/s^2. g is the acceleration of gravity and is set to be 9.81 m/s^2. $grade$ is the road gradient, %. C_R is the rolling resistance coefficient. ρ_a is the air ambient density. C_D is the air resistance coefficient. A_i is the area of the vehicle cross-section, m^2. m is the total vehicle mass, kg [32]. provided model parameters of VSP model for LDVs based on empirical data, and the VSP value of LDVs can be expressed by Eq. (2).

$$VSP = v \times (1.1a + g \times grade + 0.132) + 0.000302v^3 \tag{2}$$

In this study, the effect of the slope is not considered because the experimental areas (i.e., Shanghai, China) are plain without much variation in altitude, so *grade* is set to be 0 [28]. The VSP formula for HDVs is not the same as that for LDVs due to the considerable distinctions in vehicular characteristics [33]. Referring to Ref. [33]; this study uses the following VSP calculation formula for HDVs considering vehicle weight, front-end cross-section, and other parameters regarding HDVs.

$$VSP = v \times (a + g \times grade + 0.09199) + 0.000169v^3 \tag{3}$$

Based on second-by-second speed and acceleration data, the corresponding VSP is calculated and then grouped into discrete bins, which will link to the emissions of different exhausts. Please note that even though the device can record emission and vehicle dynamic data in a high resolution (0.1s), we aggerated the data into 1s on account of variation and monitoring accuracy to obtain more reliable results. In terms of determining the number of VSP bins, two basic rules of thumb are generally adopted: (1) the emission rates in different VSP bins should be statistically different; and (2) the resolution of bins should be high enough to avoid minor VSP bins that dominate the estimate of emissions [34]. To make full use of fine-grained vehicle operating and emission data, we divide the VSP values by a step of 1 kW/t to generate the BIN partition, which can well satisfy the aforenoted two rules.

$$\forall VSP \in VSP_{\mathrm{BI.N}_i} = \begin{cases} (-\infty, -30] \\ [n-1, n), n = (-29, 29], n \in Z \\ [30, +\infty) \end{cases} \tag{4}$$

in our field data, we have collected the instantaneous vehicle dynamics, including speed and accelerations, and corresponding instantaneous emissions of exhausts (CO, HC and NO_x) detected by the OBEAS-3000 system. Using Eqs (2) and (3), the VSP at a certain time slot can be calculated based on speed and acceleration. To establish the relationship between VSP values and instantaneous exhaust emissions, we group the instantaneous emission rates (CO, HC and NO_x) by the VSP interval (every 1 kW/t) and then calculate the instantaneous emission rates in the same VSP interval to obtain representative emission rates within each VSP interval. Especially, the processes are separately conducted for LDVs and HDVs. The final results for the instantaneous emissions within different VSP intervals for LDVs and HDVs are summarized in Table 2. These results construct a relationship between the vehicle operating conditions (speed and acceleration), VSP values, and the corresponding emission rates for the different exhausts, which can be utilized for the following analysis. Particularly, there are remarkable differences in the emission rates of different exhausts in the same VSP interval, which corroborates the necessity to develop separate emission models for HDVs and LDVs.

Table 2
Instantaneous emission data for VSP at 1 kW/t partition for LDV and HDV.

VSP	LDV			HDV		
	Instantaneous emissions (mg/s)			Instantaneous emissions (mg/s)		
	CO	HC	NO_x	CO	HC	NO_x
(-∞ , -30)	4.27	0.77	0.15	111.84	13.71	18.59
[-30 , -29)	4.28	0.42	0.08	68.45	10.99	14.89
[-29 , -28)	4.62	0.59	0.15	92.02	11.37	12.18
[-28 , -27)	2.92	0.74	0.23	87.14	11.88	14.90
[-27 , -26)	2.16	0.34	0.03	101.90	13.81	17.80
[-26 , -25)	7.95	0.57	0.24	116.41	15.56	21.67
[-25 , -24)	5.72	0.60	0.27	103.48	9.40	14.62
[-24 , -23)	4.80	0.57	0.20	151.47	14.57	11.74
[-23 , -22)	2.30	0.47	0.03	150.56	14.54	22.91
[-22 , -21)	3.06	0.50	0.45	96.43	12.78	18.73
[-21 , -20)	5.05	0.72	0.26	94.08	10.62	8.31
[-20 , -19)	4.49	0.51	0.10	131.80	12.39	26.63
[-19 , -18)	5.50	0.57	0.19	70.33	9.79	14.96
[-18 , -17)	3.06	0.62	0.16	82.79	11.78	10.88
[-17 , -16)	3.78	0.55	0.15	65.97	8.61	10.20
[-16 , -15)	4.25	0.62	0.36	108.66	13.05	15.14
[-15 , -14)	5.59	0.51	0.18	83.90	13.32	22.83
[-14 , -13)	5.21	0.65	0.07	71.29	9.00	10.73
[-13 , -12)	5.19	0.72	0.13	97.78	10.85	16.90
[-12 , -11)	5.54	0.54	0.07	72.69	11.87	14.59
[-11 , -10)	4.45	0.88	0.17	78.75	9.81	17.12
[-10 , -9)	5.67	0.59	0.20	68.22	10.15	14.64
[-9 , -8)	5.45	0.57	0.18	72.19	10.51	12.09
[-8 , -7)	4.56	0.85	0.14	86.53	10.18	15.16
[-7 , -6)	5.14	0.46	0.16	63.44	11.11	15.15
[-6 , -5)	4.23	0.53	0.05	65.69	11.54	13.29
[-5 , -4)	6.22	0.95	0.24	63.83	9.04	12.25
[-4 , -3)	3.74	0.49	0.10	70.91	9.54	12.91
[-3 , -2)	3.94	0.69	0.06	64.36	8.84	10.11
[-2 , -1)	3.13	0.53	0.12	75.58	11.72	17.61
[-1 , 0)	3.31	0.59	0.08	100.49	11.19	14.50
[0 , 1)	2.24	0.42	0.02	46.95	7.29	7.44
[1 , 2)	3.56	0.65	0.07	66.88	9.38	11.09
[2 , 3)	4.09	0.60	0.16	60.13	9.35	13.09
[3 , 4)	4.67	0.71	0.09	69.81	10.73	14.52
[4 , 5)	7.24	0.80	0.22	103.63	9.79	15.63
[5 , 6)	3.90	0.56	0.14	73.96	11.21	16.24
[6 , 7)	6.92	0.81	0.21	87.71	9.40	11.86
[7 , 8)	7.82	0.84	0.10	97.53	10.64	13.26
[8 , 9)	5.62	0.69	0.22	91.18	10.45	14.83
[9 , 10)	8.96	0.82	0.41	73.50	10.37	16.70
[10 , 11)	7.27	0.67	0.16	84.97	10.50	13.36
[11 , 12)	7.68	0.75	0.30	100.07	11.69	15.73
[12 , 13)	6.60	0.77	0.18	81.80	11.77	16.48
[13 , 14)	9.29	0.85	0.38	92.66	11.56	14.74
[14 , 15)	8.99	0.89	0.23	103.44	11.97	18.88
[15 , 16)	7.95	0.72	0.14	100.01	12.36	17.27
[16 , 17)	8.22	0.95	0.18	82.90	12.08	16.32
[17 , 18)	6.14	1.19	0.26	107.68	14.08	20.35
[18 , 19)	6.66	0.86	0.23	159.31	14.13	12.92
[19 , 20)	7.74	0.80	0.32	93.99	11.32	20.34
[20 , 21)	11.87	0.94	0.32	94.69	11.43	14.51
[21 , 22)	7.01	0.79	0.22	102.21	11.87	21.39
[22 , 23)	8.85	0.86	0.28	86.06	12.50	19.13
[23 , 24)	8.89	1.05	0.26	76.94	11.99	16.88
[24 , 25)	12.19	0.93	0.23	72.89	11.73	16.74
[25 , 26)	5.82	1.00	0.26	96.07	12.32	19.84
[26 , 27)	6.91	0.81	0.20	90.50	10.95	17.97
[27 , 28)	11.08	1.01	0.33	111.83	13.61	18.04
[28 , 29)	5.73	1.82	0.55	102.11	12.49	16.47
[29 , 30)	16.03	0.97	0.32	117.23	11.97	22.59
[30 , +∞)	6.77	1.51	0.27	110.06	13.62	23.34

3. Determining the left-turn lane for mixed traffic flow

The left-turn lane at an intersection generally includes a deceleration section (traverse section) and a storage section (see Fig. 2 (a)). Vehicles complete the traverse from through to left-turn in the deceleration section and then turn left or queue to wait for the next green-light phase. Inadequate lengths of the storage section will result in two consequences, as shown in Fig. 2 (b) and (c). A large number of left-turn vehicles will cause the left-turn queue to block the adjacent straight lane, making it impassable for the through traffic, as shown in Fig. 2(b). A long queue of through traffic will block the left-turn lane, preventing left-turning vehicles from passing into the storage section, as shown in Fig. 2(c). Short left-turn lane length can cause increased conflict between left-turning and straight-

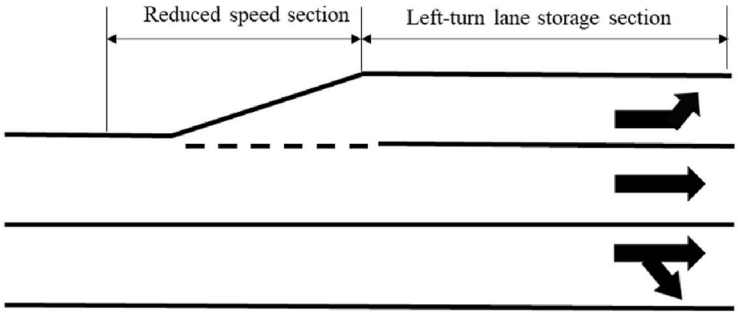

(a) Composition of the left-turn lane

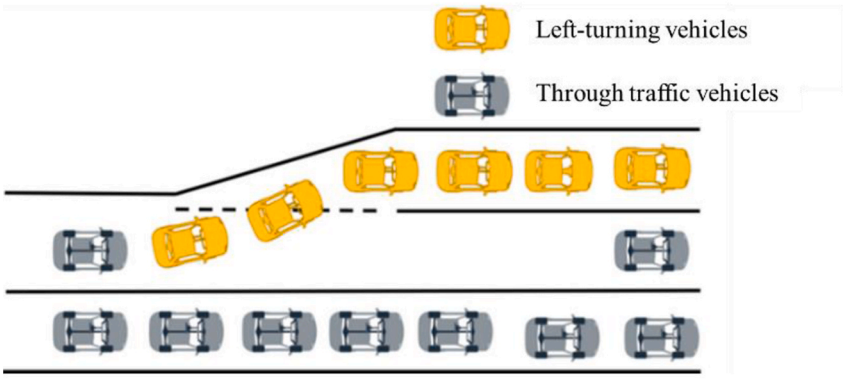

(b) Left-turning queuing vehicles obstructing through traffic

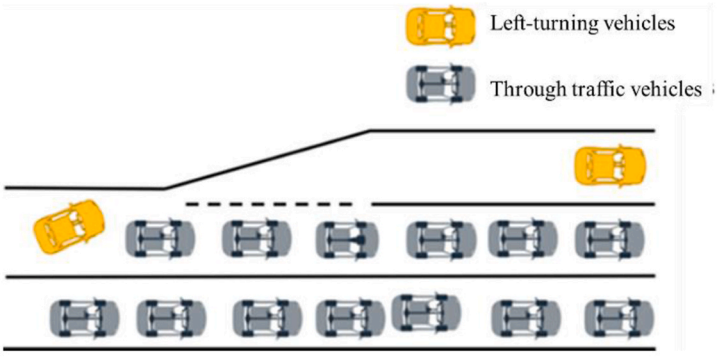

(c) Queuing of through traffic obstructing left-turning traffic

Fig. 2. Diagram showing the impact of insufficient left-turn lane storage length on traffic flow.

through vehicles, so the length of the left-turn storage section is, therefore, crucial to the operational efficiency of the intersection. Our design aim is to determine the optimal storage length of the left-turn lane for mixed traffic with different penetration rates of HDVs for reducing conflict points, traffic delays, and thus traffic emissions at the intersection. Due to the large difference in the length of HDVs and LDVs, the left-turn lane storage length for mixed traffic flow must consider not only the number of vehicles in the traffic flow but also the proportion of HDVs in the traffic flow. It is worth noting that it is implausible to directly formulate an optimization in which left-turn lane length is the decision variable and the overall traffic emission at the intersection is the objective function [15,26,27]. The reason is that the quantitative relationships between left-turn lane length and traffic emission cannot be mathematically modeled directly or indirectly. However, leveraging the validated relations between traffic delays and emissions, it is plausible to formulate an optimization model minimizing traffic delays and minimizing traffic emissions indirectly. This strategy has been adopted and validated by several relevant studies [15,16,20,26,27] and is utilized herein.

Assuming that the traffic flow on the road section consists of n different types of vehicles and the length of the vehicle type i is L_i with $L_1 < L_2 < \cdots < L_i < \cdots < L_n$. The proportion of vehicle type i is P_i and $P_1 + P_2 + \cdots + P_i + \cdots + P_n = 1$. Because the combination of two adjacent vehicles in the traffic flow is random, the probability of the combination that the preceding vehicle is the type i and the following vehicle is the type j, is P_iP_j. Then, it is easy to verify, as shown in Eq. (5).

$$\sum_{i=1}^{r}\sum_{j=1}^{r} p_i p_j = (p_1 + p_2 + \cdots + p_r)^2 = 1 \tag{5}$$

Assume t_{ij} is the time headway between vehicle type i and vehicle type j when the traffic volume reaches the capacities of a lane. We can estimate the average time headway in the mixed traffic of various vehicle types, as shown in Eq. (6).

$$H_t = \sum_{i=1}^{n}\sum_{j=1}^{n} p_i p_j t_{ij} \tag{6}$$

Based on the average time headway, the theoretical capacity of one lane for mixed traffic is

$$CP = \frac{3600}{H_t} = \frac{3600}{\sum_{i=1}^{n}\sum_{j=1}^{n} p_i p_j t_{ij}} \quad i,j = 1,2,3,\cdots,n \tag{7}$$

The above equations are genera for mixed traffic flows with several vehicle types. However, this study mainly investigates the case of two types of vehicles on account of the available emission models, namely $n = 2$. Let us assume the proportion of LDVs and HDVs are p and $1 - p$. We use subscripts l and h to denote light- and heavy-duty vehicles, respectively. It can be deduced that the capacity of a lane for mixed traffic flow is

$$CP = \frac{3600}{\sum_{i=1}^{2}\sum_{j=1}^{2} p_i p_j t_{ij}} = \frac{3600}{t_{ll}p^2 + (t_{lh} + t_{hl})p(1-p) + t_{hh}(1-p)^2} \tag{8}$$

In a mixed traffic flow, the arrival rate of left-turn vehicles at the intersection is λ (veh/h), and the maximum number of vehicles per hour that can pass the intersection at the left-turn green light phase is μ. λ is set to be less than μ. Otherwise, it will be undissipated traffic congestion. We assume that vehicle arrivals follow a Poisson distribution and time headway follows a negative exponential distribution, as most traffic flow studies did [8,9]. In this regard, this is a typical M/M/1 queuing model. As per the queueing theory, the probability that there is a queue of n_l LDVs waiting in the left-turn lane at a given time is

$$P_{nl} = p\left(1 - \frac{\lambda}{\mu}\right)\left(\frac{\lambda}{\mu}\right)^{n_l} \tag{9}$$

The probability of having n_h HDVs waiting in the left-turn lane is

$$P_{nh} = (1-p)\left(1 - \frac{\lambda}{\mu}\right)\left(\frac{\lambda}{\mu}\right)^{n_h} \tag{10}$$

The probability of fewer than N vehicles queuing in the left-turn lane is

$$P(x \le N) = 1 - \left(\frac{\lambda}{\mu}\right)^{N+1} \tag{11}$$

$$N = \left[\frac{ln(1 - P(x \le N))}{ln\left(\frac{\lambda}{\mu}\right)} - 1\right] \tag{12}$$

In the N vehicles, the number of LDVs queuing in the left-turn lane N_l is

$$N_l = Np = p \times \left[\frac{ln(1 - P(x \le N))}{ln\left(\frac{\lambda}{\mu}\right)} - 1 \right] \tag{13}$$

and the number of HDVs queuing in the left-turn lane N_h is

$$N_h = (1 - p) \times \left[\frac{ln(1 - P(x \le N))}{ln\left(\frac{\lambda}{\mu}\right)} - 1 \right] \tag{14}$$

The maximum number of vehicles per hour that can pass the intersection at the left-turn green light phase μ.

$$\mu = \frac{S_L G_L}{C} \tag{15}$$

where S_L is the hourly maximum traffic throughput of a single left-turn lane (veh/h), namely the capacity, which can be calibrated based on Eq. (8). G_L is the effective green time of the left-turn protection phase (in seconds), and C is the signal cycle length in seconds. Then, we can get Eq. (16).

$$\frac{\lambda}{\mu} = \frac{\lambda C}{S_L G_L} \tag{16}$$

In mixed traffic flows, the average length occupied by an LDV while parking is approximately 1.5 times its length, with a default value of 7.6 m. Referring to relevant literature [35], the average length occupied by an HDV L_h is related to the percentage of HDV in mixed traffic and can be approximated by Eq. (17).

$$L_h = 7.6(1 + M) = 7.6(2 - p) \tag{17}$$

To accommodate the N vehicles with N_l LDVs and N_h HDVs, the length of the stored section of the left-turn lane should be followed Eq. (18).

$$L_S = 7.6N_l + L_h N_h \tag{18}$$

Combining Eqs. (13), (14) and (18), the length of the stored section of the left-turn lane that wants to ensure no spillover in Fig. 2 (a) at the probability of P is

$$L_S = 7.6p\left[\frac{ln(1 - P)}{ln(\lambda C) - ln(S_L G_L)} - 1\right] + 7.6(2 - p)(1 - p)\left[\frac{ln(1 - P)}{ln(\lambda C) - ln(S_L G_L)} - 1\right] \tag{19}$$

The value of P denotes the probability of ensuring no spillover in the left-turn storage lane and is the empirical value that considers the tradeoff between construction costs and service levels. If the value of P is too large, the length of the left-turn storage lane will be very long, which can ensure service levels but be a waste of the lane in most periods. If the value of P is too small, there will be a high risk or probability of left-turn lane spillover. Based on the arrival rate of left-turn traffic, the signal phases and cycles in an intersection, lane capacity of left turning, and penetration rate of HDVs in the traffic flow, we can design the corresponding left-turn lane length as per Eq. (19), which is tailored for mixed traffic.

Fig. 3. Cao'an road – Jiasong north road intersection.

4. Empirical analyses based on field scenarios

To validate the effects of the proposed method on the traffic emissions of mixed traffic at intersections, we conduct an empirical analysis regarding a typical intersection with mixed traffic in Shanghai, China. We use the VISSIM simulator to simulate the traffic and obtain high-resolution vehicle trajectories before and after optimizing the left-turn lane. In the simulation, we consider motor vehicles including LDVs and HDVs, but do not consider micro-mobility such as bicycles and scooters, which are out of the scope of this study. The intersection of Cao'an Road and North Jiasong Road (see Fig. 3) was chosen for the case study. The reasons for selecting the intersection are 1) the intersection has a high traffic flow with congestion in the morning and especially has high left-turn traffic flow; 2) all inlet lanes from four directions of the intersection have left-turn lanes; 3) the traffic flow at the intersection has many HDVs and is a typical mixed traffic flow. At this intersection, Cao'an Road is a two-way 12-lane urban road, with each inlet lane comprising two left-turn-only lanes, three through lanes, and one right-turn lane. North Jiasong Road is a six-lane urban road in both directions, which includes one left-turn lane, one straight-through lane, and one right-turn lane. A bird's view of the intersection is shown in Fig. 3. To reflect the real traffic flow characteristics in the intersection appropriately, we have conducted field surveys in the morning peak hours at the intersection for one week (from Monday to Friday, 7:30 a.m.-8:30 a.m.). Drones were used to record video above the intersection. Details about traffic flow in terms of traffic volumes and penetration rate of HDVs were extracted manually from the recorded videos. We did not apply computer vision techniques as manual counting is more accurate even though time-consuming. The details of the traffic flow are summarized in Table 3. Please note that we average the data from five consecutive days to get the representative values.

The traffic volumes in VISSIM are inputted according to the traffic volumes at the intersections of the field survey, and the road network is built according to the actual construction of the intersections in the original scenario of the simulation. Based on the field research, the VISSIM simulation platform is built with the intersections taken in the field as the base map (see Fig. 4).

The total number of LDVs in the morning peak hour was 4062, representing 85.91% of the total traffic, while HDVs were 666, representing 14.09% of the total traffic. For different directions, the proportion of LDVs ranged from 76.43% to 95.18%, while the proportion of HDVs ranged from 4.82% to 23.57%. It can be observed that the penetration rate of HDVs in different directions is distinct. Meanwhile, the traffic volumes from and to different directions have considerable variation as well. As indicated by the results of the field survey, there are considerable delays in different import lanes. We compare the traffic emissions and efficiency at the intersections in original and optimized scenarios. In the original scenario, we use the real and current settings about the length of left-turn lanes in different directions at the intersections. In the optimized scenario, we use our proposed method to determine the length of left-turn lanes in different directions according to the traffic volume, the penetration rate of HDVs, and signal timing. The lengths of left-turn lanes in different directions in two scenarios are summarized in Table 4. We simulate the case of morning peak hours as per our field survey data. In the VISSIM simulation, the velocity and acceleration of each vehicle are recorded and outputted at the frequency of 1 s. We record the vehicles' information during the period from the time frame when they arrive 200 m away from the stop line of the entrance lane to the time frame when they leave 200 m away from the stop line of the exit lane. Based on these data, we use the developed instantaneous emission models for LDV and HDV in Section 2.2 to estimate the emissions of CO, HC, and NO_x of each vehicle crossing the intersections. In this manner, the emissions of all vehicles crossing the intersection in the two scenarios can be directly quantified and compared. We repeat the simulation five times to eliminate the potential biases due to randomness. The mean values of emissions in the five simulations are used for representatives.

The results of the emissions in the two comparative scenarios are summarized in Table 4. The results show that the CO, HC, and NO_x emissions of all traffic, including LDVs and HDVs at the intersections, are substantially reduced at the intersection in the optimized scenario. More specifically, the CO emission in the optimized scenario decreases by 34.43% as compared to the original scenario, which is a significant improvement. The same goes for HC and NO_x emissions, which reduce by 29.77% and 30.42% in the optimized scenario, respectively. The results indicate that the proposed method for improving left-turn lane settings can cut down traffic emissions considerably in terms of CO, HC, and NO_x.

More importantly, the emission patterns of LDV and HDV show divergences. It can be observed in Table 5 that the percentage of HDV in the mixed traffic flow is much smaller than that of LDV. The proportion of LDV in the traffic flow from different directions

Table 3
Morning peak-hour Traffic volume at the investigated intersection.

Entrance	Turning	LDV	HDV	Percentage of LDV	Percentage of HDV	Average delay(s)	Max. delay(s)	Max. Queue length(m)
West Entrance	Left	45	21	95.18%	4.82%	81.5	197.8	103.2
	Right turn	59	7	89.39%	10.61%	11.2	29.1	0
	Straight	737	137	84.32%	15.68%	72.6	174.2	106.2
East Entrance	Left	313	31	90.99%	9.01%	62.9	190.1	57.6
	Right turn	231	61	79.11%	20.89%	1.5	7.4	0
	Straight	563	72	88.66%	11.34%	83.7	183.5	154.5
North Entrance	Left	253	45	84.90%	15.10%	57.7	146.5	124.4
	Right turn	160	27	85.56%	14.44%	3.5	16.9	13.2
	Straight	597	85	87.54%	12.46%	66.7	164.0	53.9
South Entrance	Left	207	58	78.11%	21.89%	88.9	191.1	169.2
	Right turn	120	37	76.43%	23.57%	28.5	83.0	90.2
	Straight	407	85	82.72%	17.28%	75.3	186.8	172.7
Total number vehicles		4062	666	85.91%	14.09%			

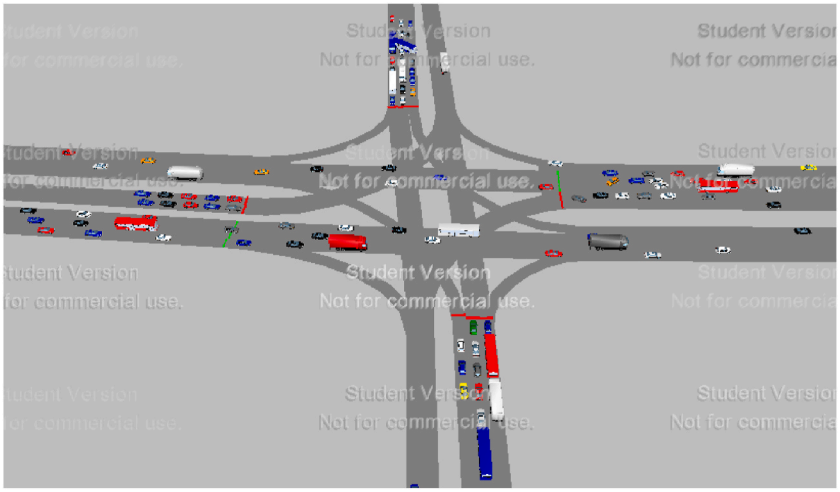

Fig. 4. Simulation scenario in VISSIM.

Table 4
Storage length of the left-turn lane.

Directions	Length of the left-turn lane in original scenario (m)	Length of the left-turn lane in optimized scenario (m)
West Entrance t	70	120
East Entrance	70	93
North Entrance	50	122
South Entrance	50	63

varies from 76.43% to 95.18%, with an average value of 85.91%. The percent of HDV from different directions varies from 4.82% to 23.57%, with a mean of 14.09%. However, the emission results in Table 4 show that in the original scenario, the LDVs merely contribute 27.86% of CO, 31.61% of HC, and 5.67% of NO_x, which is not proportional to the percentage of LDV in traffic volumes. In contrast, HDVs produce 72.14% of CO, 68.39% of HC, and 94.33% of NO_x in the studied intersection, even though they merely take up 14.09% of traffic flows. The same phenomenon is observed in the optimized scenario. HDVs contribute the most emissions of CO, HC, and NO_x, although the percentage of HDVs is not large. These results imply the necessity of specific measures for reducing the traffic emissions of traffic flow with only LDVs, and mixed traffic flow with HDVs, as well as the merits of the proposed method for mixed traffic. For LDV, the CO emissions reduce by 33.74% in the optimized scenario as compared to the original scenario. A similar reduction in CO emissions (34.7%) for HDVs is also found. The HC emissions of LDVs decrease by 17.78%, but the reduction in the HC emissions for HDVs is more notable (35.31%). The NO_x emissions for LDVs reduce by 27.93% in the optimized scenario, similar to the reduction of NO_x emissions for HDVs (30.57%). The results demonstrate that the optimization of the left-turn lane has similar impacts on the reduction of CO and NO_x emissions for LDVs and HDVs, but has a more remarkable influence on the HC emissions for HDVs compared to LDVs.

To further validate the reliability of the proposed method to determine the storage length of left-turn lanes properly, we have enumerated the relationship between the storage length of the left-turn lane and corresponding traffic emission in the north import directions at an increment of 25 m. The results are summarized in Table 5. It can be seen that the emissions of CO, HC, and NO_x from LDVs decrease with the increase of left-turn lane length firstly, reach a swale at the length of 125 m, and then increases with a longer left-turn lane. The same pattern can be observed for HDV with differences in absolute values. Interestingly, the emissions, to some extent, increase with a longer left turn, which seems counterintuitive but rational. The reason found from observing the trajectories of vehicles is that straight-through traffic would use the left-turn lane to take over preceding vehicles and cut into the straight-through lanes when the left-turn lane is rather long, as demonstrated in Fig. 5. These behaviors will increase the conflicting points in the traffic and result in traffic oscillations (deceleration and acceleration behavior) due to cut-in behaviors, which will lead to higher vehicle emissions. More importantly, the best length for the left-turn lane is around 125 m in the enumeration, which is highly aligned with the theoretically derived value of 122 m based on our proposed method in Table 6. These corroborate the validity and ability of the proposed method to determine the optimized left-turn storage length for mixed traffic properly.

The setting of the left-turn lane storage not only affects emissions but also traffic efficiency at the intersection in terms of travel time and delays. Therefore, we compare the changes in the traffic efficiency before and after optimizing the left-turn lane in terms of average travel delay, maximum delay, and maximum queue length in different directions. The results are summarized in Table 7. The average traffic delays in different entrance directions after optimization reduces by 14.61% (West), 2.68% (East), 16.67% (North), and 21.09% (South). The maximum delays of vehicles from different directions reduce by 4.73%–9.05%. The maximum queue lengths in different directions decrease significantly by 37.02%, 79.42%, and 39.09%. The improvements are mainly attributed to avoiding the

Table 5
Comparison of emissions before and after optimization.

		Original scenario		Optimized scenario		Emission reduction
		Overall emission (g/h)	The proportion of different vehicle types	Overall emission (g/h)	The proportion of different vehicle types	
All vehicles	CO	26031.94		17068.5		34.43%
	HC	3731.64		2620.74		29.77%
	NO_x	3453.18		2402.58		30.42%
LDV	CO	7252.14	27.86%	4804.98	28.15%	33.74%
	HC	1179.72	31.61%	970.02	37.01%	17.78%
	NO_x	195.90	5.67%	141.18	5.88%	27.9%
HDV	CO	18779.80	72.14%	12263.52	71.85%	34.70%
	HC	2551.92	68.39%	1650.72	62.99%	35.31%
	NO_x	3257.28	94.33%	2261.40	94.12%	30.57%

Note: The proportion of different vehicle types is calculated by the emissions of one exhaust from a vehicle type (e.g., LDS) divided by the emission of one exhaust from all vehicles.

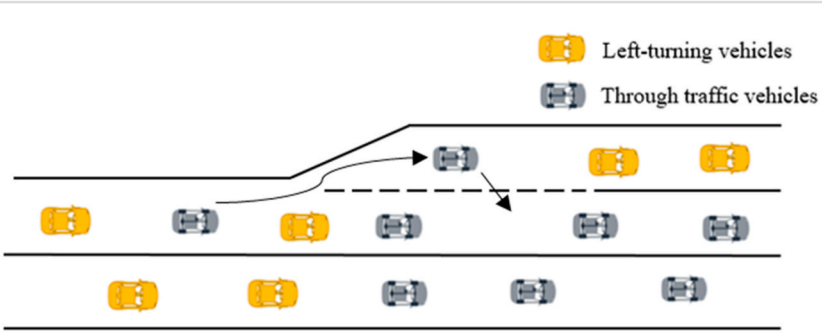

Fig. 5. Through traffic uses left-turn storage lane to take over.

Table 6
The effects of left-turn lane storage length on traffic emission in the north import.

	LDV			HDV		
Length of left-turn lane	CO (g/h)	HC (g/h)	NO_x (g/h)	CO (g/h)	HC (g/h)	NO_x (g/h)
Original scenario (50 m)	1802.9	293.3	48.7	4426.4	601.5	767.7
75 m	1514.0	297.8	42.2	3863.1	523.6	702.1
100 m	1437.6	286.7	41.0	3794.3	513.3	695.6
125 m	1194.5	241.1	35.1	2890.5	389.1	533.0
150 m	1536.8	305.2	44.9	4125.5	553.5	757.0
175 m	1486.9	296.9	43.4	3714.8	496.5	687.4
200 m	1539.1	306.6	45.3	3683.3	492.2	681.7

Note: We use the north import direction as the representative and repeating the validation process in other directions can find similar conclusions, which are not elaborated in case of redundancy.

Table 7
Comparison of emissions under emission optimization and delay optimization.

	West import	East Import	North Import	South Import
ORS -Average delay(s)	69.16	59.19	54.27	71.2
OPS -Average delay(s)	59.05	57.6	45.23	56.19
Reduction percentage	14.61%	2.68%	16.67%	21.09%
ORS-Maximum delay(s)	197.8	190.1	164	186.8
OPS-Maximum delay(s)	181.9	181.1	155.9	169.9
Reduction percentage	8.04%	4.73%	4.94%	9.05%
ORS-Maximum queue length(m)	106.2	154.5	124.4	172.7
OPS-Maximum queue length(m)	57.8	97.3	25.6	105.2
Reduction percentage	45.57%	37.02%	79.42%	39.09%

Note: ORS and OPS denote the original scenario and optimized scenario, respectively.

harmful scenarios demonstrated in Fig. 2 by providing appropriate storage lanes for left-turn vehicles. The results demonstrate that the proposed method can reduce travel delays and queues considerably and generate benefits in traffic efficiency. Although heavy vehicles only account for 13–18% of the vehicle count in the intersection, they generate more than 70% of CO emissions, over 65% of HC emissions, and more than 90% of NOx emissions from all heavy vehicles.

5. Conclusions

This study investigates the optimization and emission analysis regarding the effects of left-turn lanes on the emissions (CO, HC and NO_x) of mixed traffic flow with both LDVs and HDVs at urban intersections. High-resolution field emission and vehicle operating data of LDVs and HDVs in real urban contexts are collected and used to establish instantaneous emission models for HDVs and LDVs regarding CO, HC and NO_x. Meanwhile, a tailored model is formulated to determine the optimal left-turn lane length based on queueing theories and the penetration rate of HDVs. The proposed method is validated using an empirical case study combining established emission models and VISSIM simulation tools and based on field data in a typical intersection.

The results show that the proposed method can reduce the CO, HC and NO_x emissions at the intersection by around 30% as compared to the original scenario. An enumeration process is conducted to validate further the ability of the proposed method to determine the proper length of left-turn lanes. The optimization of the left-turn lane has similar impacts on the reduction of CO and NO_x emissions for LDVs and HDVs but has a more remarkable influence on the HC emissions for HDVs as compared to LDVs. It is found

that HDVs contribute to most of CO, HC, and NO_x emissions at the intersection whilst they take up a small percentage of the traffic flow. The proposed method can also improve traffic efficiency at the intersection by reducing travel delays and queuing, as evidenced by empirical analysis results. This study establishes the instantaneous emission model for mixed traffic flow and provides a model basis for calculating traffic emissions from mixed traffic flows. Moreover, the results provide useful guidance and design methods for transportation designers to optimize and improve the left-turn lane configuration to alleviate traffic congestion and reduce traffic emissions at urban intersections.

Compared to former studies, this study offers several unique contributions regarding the impact of left-turn lanes on traffic emissions. Firstly, we collected high-resolution field emission and vehicle operating data for both LDVs and HDVs, providing a comprehensive understanding and modelling of the emissions of LDVs and HDVs in different operation conditions, which are essential for analyzing emissions of mixed traffic flow. Secondly, we formulated a tailored model to determine the optimal left-turn lane length, which takes into account queueing theories and the penetration rate of HDVs. Finally, the proposed method was validated using an empirical case study, providing evidence of its effectiveness in reducing emissions and improving traffic efficiency.

Nevertheless, there are several limitations that can be further investigated in future work. Firstly, it is tough to directly formulate quantitative models about emissions at the traffic flow level in the optimization model of left-turn lanes, as the change of left-turn lane design will influence several aspects and a lot of vehicles rather than a certain vehicle. It will be interesting work to develop a quantitative method for reflecting the relationship between changes in traffic flow characteristics and corresponding emissions. In this regard, the objective function of the optimization will be more straightforward. Moreover, this study focuses on the left-turn lane design and takes the signal timing setting at the intersection as the default input. However, the signal timing can be optimized and controlled to facilitate traffic efficiency as well, which a load of literature has been doing. It is an interesting future work to jointly optimize lane configuration design and signal timing at the intersection, which is expected to have more remarked benefits. Last but not least, our emission models are established based on the field emission data of three representative vehicles due to data limitations and the high expense of collecting data from various LDVs and HDVs. Collecting more field emission data will always be beneficial for improving the instantaneous emission models and analysis accuracy in relevant studies.

Author contribution statement

Jieyu Fan: Kun Gao: Conceived and designed the experiments; Performed the experiments; Analyzed and interpreted the data; Wrote the paper. Aoyong Li: Performed the experiments; Analyzed and interpreted the data; Contributed reagents, materials, analysis tools or data; Wrote the paper. Anugrah Ilahi: Performed the experiments; Analyzed and interpreted the data; Wrote the paper.

Data availability statement

The authors do not have permission to share data.

Declaration of competing interest

The authors declare that they have no known competing financial interests or personal relationships that could have appeared to influence the work reported in this paper.

Acknowledgment

The authors are grateful to the Area of Advance Transport and AI Center (CHAIR) at the Chalmers University of Technology for funding this research.

References

[1] X. Qu, Z. Zeng, K. Wang, S. Wang, Replacing urban trucks via ground–air cooperation, Commun. Transport. Res. 2 (2022), 100080.
[2] P. Miklautsch, M. Woschank, A framework of measures to mitigate greenhouse gas emissions in freight transport: systematic literature review from a Manufacturer's perspective, J. Clean. Prod. (2022) 132883.
[3] L.G. Costa, Y.-C. Chang, T.B. Cole, Developmental neurotoxicity of traffic-related air pollution: focus on autism, Curr. Environ. Health Rep. 4 (2) (2017) 156–165.
[4] X. Qu, S. Wang, D. Niemeier, On the urban-rural bus transit system with passenger-freight mixed flow, Commun. Transport. Res. 2 (2022), 100054.
[5] E. Long, C. Carlsten, Controlled human exposure to diesel exhaust: results illuminate health effects of traffic-related air pollution and inform future directions, Part. Fibre Toxicol. 19 (1) (2022) 11.
[6] A. Jamshidnejad, I. Papamichail, M. Papageorgiou, B. De Schutter, A mesoscopic integrated urban traffic flow-emission model, Transport. Res. C Emerg. Technol. 75 (2017) 45–83.
[7] B. Saud, G. Paudel, The threat of ambient air pollution in Kathmandu, Nepal, J. Environ. Public Health 2018 (2018), 1504591.
[8] K. Gao, Y. Yang, G. Jorge, X. Qu, Data-driven Interpretation on interactive and nonlinear effects of the correlated built environment on shared mobility, J. Transport Geogr. (2023) 1–16.
[9] J. Zhu, S. Easa, K. Gao, Merging control strategies of connected and autonomous vehicles at freeway on-ramps: a comprehensive review, J. Intell. Connect. Veh. 5 (2) (2022) 99–111.
[10] O.V. Lozhkina, V.N. Lozhkin, Estimation of nitrogen oxides emissions from petrol and diesel passenger cars by means of on-board monitoring: effect of vehicle speed, vehicle technology, engine type on emission rates, Transport. Res. Transport Environ. 47 (2016) 251–264.
[11] S. Zhang, Y. Wu, H. Liu, R. Huang, P. Un, Y. Zhou, L. Fu, J. Hao, Real-world fuel consumption and CO2 (carbon dioxide) emissions by driving conditions for light-duty passenger vehicles in China, Energy 69 (2014) 247–257.

[12] K. Zhang, S. Batterman, F. Dion, Vehicle emissions in congestion: comparison of work zone, rush hour and free-flow conditions, Atmos. Environ. 45 (11) (2011) 1929–1939.
[13] T. Lee, H.C. Frey, Evaluation of representativeness of site-specific fuel-based vehicle emission factors for route average emissions, Environ. Sci. Technol. 46 (12) (2012) 6867–6873.
[14] M.K. Robinson, B.A. Holmén, Hybrid-electric passenger car energy utilization and emissions: relationships for real-world driving conditions that account for road grade, Sci. Total Environ. 738 (2020), 139692.
[15] W.F. Bremer, M.V. Chitturi, Y. Song, B.R. Claros, A.R. Bill, D.A. Noyce, Design Standards for Unobstructed Sight Lines at Left-Turn Lanes, Department of Transportation, Minnesota, 2019.
[16] A.J. Calle-Laguna, J. Du, H.A. Rakha, Computing optimum traffic signal cycle length considering vehicle delay and fuel consumption, Transp. Res. Interdiscip. Perspect. 3 (2019), 100021.
[17] K. Gao, Y. Yang, X. Qu, Examining nonlinear and interaction effects of multiple determinants on airline travel satisfaction, Transport. Res. Transport Environ. 97 (2021), 102957.
[18] F. Corriere, G. Rizzo, M. Guerrieri, Estimation of Air Pollutant Emissions in "Turbo" and in Conventional Roundabouts, *Applied Mechanics and Materials*, Trans Tech Publ, 2013, pp. 597–604.
[19] L. Vasconcelos, A.B. Silva, Á.M. Seco, P. Fernandes, M.C. Coelho, Turboroundabouts: multicriterion assessment of intersection capacity, safety, and emissions, Transport. Res. Rec. 2402 (1) (2014) 28–37.
[20] E. Nyame-Baafi, C.A. Adams, K.K. Osei, Volume warrants for major and minor roads left-turning traffic lanes at unsignalized T-intersections: a case study using VISSIM modelling, J. Traffic Transport. Eng. 5 (5) (2018) 417–428.
[21] K. Gao, M. Shao, K.W. Axhausen, L. Sun, H. Tu, Y. Wang, Inertia Effects of past behavior in commuting modal shift behavior: interactions, variations and implications for demand estimation, Transportation (2022) 1–35.
[22] M. Guo, S. Chen, J. Zhang, J. Meng, Environment Kuznets curve in transport sector's carbon emission: evidence from China, J. Clean. Prod. 371 (2022), 133504.
[23] S. Kikuchi, N. Kronprasert, Determining lengths of left-turn lanes at signalized intersections under different left-turn signal schemes, Transport. Res. Rec. 2195 (1) (2010) 70–81.
[24] R. Yang, W. Zhu, Study on the operation of left-turn vehicles at signalized intersections based on the car-following model, in: 2021 China Automation Congress (CAC), IEEE, 2021, pp. 4892–4897.
[25] B. Feng, M. Zheng, Y. Liu, Optimization of signal timing for the contraflow left-turn lane at signalized intersections based on delay analysis, Sustainability 15 (8) (2023) 6477.
[26] X. Bing, Y. Jiang, C. Zhang, Y. Zhang, J. Lu, Effects of intersection lane configuration on traffic emissions, Adv. Transport. Stud. (32) (2014).
[27] R. Yao, H. Michael Zhang, Optimal allocation of lane space and green splits of isolated signalized intersections with short left-turn lanes, J. Transport. Eng. 139 (7) (2013) 667–677.
[28] J. Fan, K. Gao, Y. Xing, J. Lu, Evaluating the effects of one-way traffic management on different vehicle exhaust emissions using an integrated approach, J. Adv. Transport. 2019 (2019) 1–11.
[29] N. Zacharof, U. Tietge, V. Franco, P. Mock, Type approval and real-world CO2 and NOx emissions from EU light commercial vehicles, Energy Pol. 97 (2016) 540–548.
[30] F. Rosero, N. Fonseca, J.-M. López, J. Casanova, Effects of passenger load, road grade, and congestion level on real-world fuel consumption and emissions from compressed natural gas and diesel urban buses, Appl. Energy 282 (2021), 116195.
[31] H. Perugu, Emission modelling of light-duty vehicles in India using the revamped VSP-based MOVES model: the case study of Hyderabad, Transport. Res. Transport Environ. 68 (2019) 150–163.
[32] D.W. Wyatt, H. Li, J. Tate, Examining the Influence of Road Grade on Vehicle Specific Power (VSP) and Carbon Dioxide (CO 2) Emission over a Real-World Driving Cycle, SAE Technical Paper, 2013.
[33] M. Barth, T. Younglove, G. Scora, Development of a Heavy-Duty Diesel Modal Emissions and Fuel Consumption Model, Institute of Transportation Studies, UC Berkeley, 2005.
[34] H. Wang, L. Fu, Developing a high-resolution vehicular emission inventory by integrating an emission model and a traffic model: Part 1—modeling fuel consumption and emissions based on speed and vehicle-specific power, J. Air Waste Manag. Assoc. 60 (12) (2010) 1463–1470.
[35] M. Nourinejad, A. Wenneman, K.N. Habib, M.J. Roorda, Truck parking in urban areas: application of choice modelling within traffic microsimulation, Transport. Res. Pol. Pract. 64 (2014) 54–64.